# Time- and Space-Resolved Optical Probing of Femtosecond-Laser-Driven Shock Waves in Aluminum

R. Evans,* A. D. Badger, F. Falliès, M. Mahdieh, and T. A. Hall
*Physics Department, University of Essex, Colchester, Essex, United Kingdom*

P. Audebert, J.-P. Geindre, and J.-C. Gauthier
*Laboratoire pour l'Utilisation des Lasers Intenses, Ecole Polytechnique, 91128 Palaiseau, France*

A. Mysyrowicz, G. Grillon, and A. Antonetti
*Laboratoire d'Optique Appliquée, Batterie de l'Yvette, 91120 Palaiseau, France*
(Received 26 June 1996)

We present the first measurements of particle velocity histories at the interface between an aluminum sample shocked by a 120 fs laser-driven pressure pulse and a fused silica window. Frequency-domain interferometry is used to provide space- and time-resolved measurements of the phase shift of a pair of probe pulses backscattered at the shocked interface. Pressures of 1–3 Mbar are inferred from the simultaneous measurement of the particle and shock velocities along the aluminum Hugoniot curve for $\sim 10^{14}$ W/cm$^2$ laser irradiances. [S0031-9007(96)01443-3]

PACS numbers: 52.50.Jm, 52.35.Tc, 52.70.Kz

Shock waves driven by nanosecond duration laser pulses have been exploited extensively for many years [1] in order to generate and observe matter under extreme conditions of density, temperature, and pressure [2]. When a thin layer of a solid material is heated rapidly to a temperature of 100–1000 eV, a supersonic heat wave propagates in the bulk of the target material, driven by thermal conduction. The shock wave overtakes the heat wave when the conduction front has slowed down to approximately the sound velocity. This physical situation is now a classical problem of the physics of hydrodynamic phenomena [3]. Shock waves in solids are characterized by a sharp discontinuity in the thermodynamic variables of the material. Thermal equilibrium is assumed between the electrons and the ions along the line of thermodynamic states where mass, momentum, and energy are simultaneously conserved (the Hugoniot curve). The electron-ion thermal equilibration time is typically $\sim 10$ ps because of the relatively high temperatures (1–10 eV) associated with strong laser-produced shocks. Therefore a new nonequilibrium situation occurs if much shorter laser pulses are used. In fact, some evidence for nonequilibrium between electron and ions has been demonstrated recently in experiments using shock waves driven in silicon by laser pulses even in the nanosecond regime [4,5].

With the advent of intense femtosecond lasers, it is now possible to observe these phenomena with increased temporal resolution. Intense femtosecond irradiation of a solid surface creates huge transient internal pressures ($P \approx 10$ Mbar) in the absorption region because the lattice is heated much faster than thermal expansion can occur. In such a situation, a heat front propagates first into the solid over typical distances of 100–200 nm, depending on the laser irradiance [6], and decays ultimately in a shock wave when hydrodynamic phenomena come into play. Recently, experiments have reported ionization and phase modulation between a pump and a probe beam in a glass target driven by a 700 fs laser pulse [7], as well as the time-resolved probing of electron thermal transport using a 100 fs laser pulse [8]. In these pump-probe optical studies of transparent materials, the plasma formation and the role of the nonlinear heat flow on the plasma electronic transport and optical properties were primarily investigated. We depart from these earlier studies by addressing experimentally the yet unexplored problem of subpicosecond laser-driven shock propagation in solids.

To probe the laser-driven shock waves, we use the technique of frequency-domain interferometry [9,10]. The shock-load pulse is obtained from a plasma produced by a Ti:sapphire laser oscillator-amplifier system providing a laser pulse of 120 fs duration, at $\lambda = 800$ nm, with energies up to 30 mJ. This pump pulse is focused onto the target by a $f/16$ fused silica lens. Apertures inserted in the laser beam path produce a focal spot with a diameter $\sim 100$ $\mu$m (FWHM); laser intensities on target are in the $\sim 10^{14}$ W/cm$^2$ range. The laser system is equipped with a specially designed doublet stretcher [11] to compensate for third and fourth order phase errors. In this way, an intensity contrast ratio of $10^{-6}$ is obtained 1 ps before the peak intensity, as measured by third-order autocorrelation techniques. A 120 fs probe pulse at 800 nm with energies $\sim 10$ $\mu$J is also used. This probe pulse is then passed through a Michelson interferometer to produce a pair of collinear probe pulses separated by 18 ps.

The targets used in these experiments consisted of aluminum layers of various thicknesses (10–400 nm) coated onto 2 mm thick fused silica substrates as shown schematically in Fig. 1. The fused quartz target is mounted

  

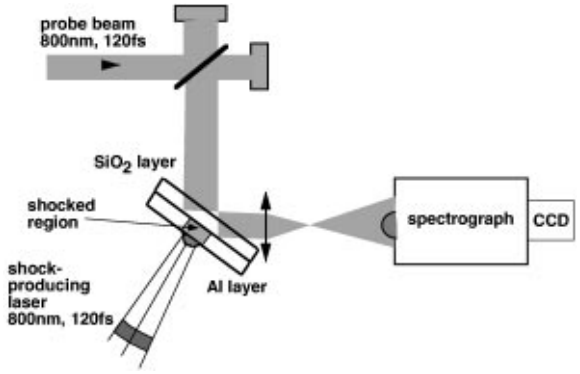


FIG. 1. Schematic view of the experimental arrangement.

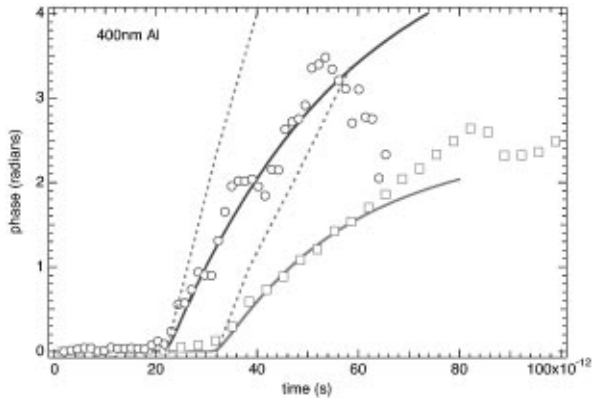


FIG. 2. Measured phase shift at the center of the focal spot as a function of time after the pump laser for a 400 nm Al layer. Circles: $2.6 \times 10^{14}$ W/cm$^2$, squares: $7.7 \times 10^{13}$ W/cm$^2$ laser intensity. Solid lines: MULTI simulations of the phase shift due to the interface. Dash-dotted line: phase calculated for the shock wave front in silica.

on a computer-driven translation stage so that each laser shot irradiates a fresh part of the target. The main laser pulse is incident on the front side of the aluminum layer at near-normal incidence (3.5°); the probe pulses are incident at 10° onto the rear side of the fused silica substrate. The relative timing between the main pulse and the two probe pulses can be varied (while keeping the probe pulse separation constant) using a computer controlled timing slide. The probe beam is partially focused onto the corresponding area of the aluminum rear surface to a spot diameter $\sim$200 $\mu$m (FWHM). This defocusing is chosen to encompass the whole region affected by the plasma producing pulse and to avoid optical damage or nonlinear effects in its own right. The reflected probe light from the aluminum layer is imaged onto the entrance slit of a 1 m focal length Czerny-Turner spectrograph with a magnification of 23. The output of the spectrograph is recorded by a charge coupled device camera and the image digitized on-line by a personal computer.

Details on the frequency-domain interferometric technique are given elsewhere [9]. This technique enables us to measure both the amplitude and the phase shift difference induced by a change of the optical properties of a perturbed material between a pair of femtosecond probe pulses with simultaneously high spatial and temporal resolutions in 2D [12,13]. Very small changes in phase ($10^{-3}$ rad) can be measured [9,10]. From the onset of the phase shift and a good knowledge of the time zero, which is obtained with a very thin tracer (10 nm) layer on each target, it is possible to measure the shock transit time across the aluminum layer very accurately. Immediately before each plasma shot, a reference with only the probe pulses present is taken to establish the fringe visibility, period, and target surface quality. All targets are coated with an antireflection film on their rear surface to suppress probe light reflection and spurious interferences in the transparent substrate that would decrease the fringe visibility.

Figure 2 shows the temporal variations of the phase for an aluminum layer thickness of 400 nm and two laser irradiances of $7.7 \times 10^{13}$ and $2.6 \times 10^{14}$ W/cm$^2$. The time zero on all plots is the time at which the first nonzero phase is observed for the thin (10 nm) tracer layer. We obtained similar results for an aluminum thickness of 260 nm. These thicknesses were chosen to ensure that the aluminum/silica interface was not perturbed by the decaying heat conduction wave during the observation time interval and for the laser irradiances that we have used [6]. Experimental results clearly show that after a time delay corresponding to the propagation time of the shock wave in the aluminum layer, there is a sharp bend of the phase signal at shock breakout, followed by a steady increase of the phase. At an irradiance of $2.6 \times 10^{14}$ W/cm$^2$ (open circles in Fig. 2), there is a strong negative perturbation of the phase signal at 35 ps after shock breakout for the 400 nm layer. For the 260 nm layer case, this perturbation occurs at 15 ps after shock breakout. At much higher irradiances, strong absorption of the probe pulse by a plasma formed at the quartz/aluminum interface [7,8] is observed, precluding any reflection phase measurements.

There are three possible contributions to the phase change, (1) changes in the optical properties of the reflecting surface, (2) motion of the reflecting surface, and (3) changes in the refractive index of the material between the reflecting surface and the observer [13]. This last contribution can be easily taken into account if the reflection is from a very steep front and the shock wave interactions in the fused quartz material are either negligible or can be calculated adequately [14]. Measurements of the phase shift for both $S$ and $P$ polarizations show only a small difference for the first 3 ps after the arrival of the shock. This implies that, at these times, the density scale length of the aluminum plasma at the interface is very much shorter than the laser wavelength [13]. We can easily calculate the phase shift associated with the motion of the reflecting surface. For the simple case of a mirror moving with speed $u$, through a medium of refractive index $n$, when viewed at an angle

$\theta$, the Doppler phase shift will give

$$d\Phi/dt = 2\omega_0(u/c)n\cos\theta,$$

where $\omega_0$ is the frequency of the probe light and $d\Phi/dt$ is the rate of change of phase of the probe pulse.

We have modeled these experiments using an improved version of the 1D Lagrangian radiative hydrodynamic code MULTI [15]. It has been modified to include an electromagnetic wave solver for the incident laser radiation, the SESAME equation of state [16], and an adequate treatment of electron-ion transport and relaxation [17]. This code has been cross-checked, with aluminum as a target material, against recent laser absorption measurements and LASNEX simulations [18] performed under similar conditions of laser irradiances and pulse durations. We used a simple dielectric multilayer reflection code as a postprocessor to MULTI, which allowed the effects of the changes in the optical properties (this will be discussed at length elsewhere) and the Doppler motion on the reflectivity and phase of the probe pulses to be modeled. Here we assumed a negligible contribution to the calculated phase shift of the variation of the index of refraction of the substrate due to the density discontinuity ($\rho/\rho_s \approx 2$) associated to the shock front in silica [14]. This is justified by the small thickness ($\sim$200 nm) of the shocked region in silica, deduced from the simulations.

Figure 2 shows the calculated phase using the postprocessor on the MULTI output for the 400 nm layer. This is compared with the experimental data for the same laser irradiance. Similar results are obtained for an aluminum layer of 260 nm. The measured shock breakout time and, furthermore, the phase variation due to the interface motion are well reproduced by the simulations. However, the experiment shows early (between 2 and 8 ps before shock breakout) phase features where the simulations show zero phase. This cannot be attributed to radiative preheat because our radiative hydrodynamic simulations show this effect to be negligible in our irradiance conditions. Hot electron penetration in the silica layer can also perturb the measured phase even though the calculated penetration depth is found to be very small compared to the Al thicknesses for any reasonable electron energy at these low irradiances [19]. We note that the simulations do not reproduce the sharp falloff of the phase at late times observed at larger irradiance. Under the present irradiation conditions, we emphasize that the calculated electron temperature in the wake of the shock front is too low, $\sim$0.5 eV, to produce any appreciable ionization in the quartz substrate. This evidence strongly suggests that we are measuring the phase and reflectivity of the aluminum-fused silica interface during and after the passage of the shock. Indeed, also shown in Fig. 2 is the calculated Doppler phase shift which would be associated to the propagation of the shock front in silica. We clearly see that the shock velocity in $SiO_2$ is very much larger than the interface velocity, as expected from the known equation of state of silica [20].

The determination of the equation of state of shocked materials requires the simultaneous measurement of the shock velocity and of an additional parameter such as, e.g., the particle (fluid) velocity [2]. By subtracting the shock breakout times measured for the same laser intensity and the two aluminum layer thicknesses, we obtain simultaneously the shock velocity and the interface velocity for given laser irradiation conditions. After correcting for the small shock impedance mismatch at the $Al/SiO_2$ interface, results are plotted in Fig. 3 together with the SESAME (3717) Hugoniot curve for aluminum. Horizontal error bars reflect the accuracy of the slope measurements of the phase shift at shock breakout together with the small ($\sim$8%) variation of the interface velocity due to the decay of the shock pressure along the 140 nm thickness difference between the two layers. Because the propagation distance of the pressure pulse in the target during the laser pulse duration is much smaller than the target thickness, strongly decaying shocks are expected to be produced. This is shown in the inset of Fig. 3 where we have plotted the calculated shock pressure as a function of time for the two laser intensities. Pressures at the interface deduced from the velocity measurements are $0.95 \pm 0.15$ Mbar and $2.55 \pm 0.5$ Mbar for $7.7 \times 10^{13}$ W/cm$^2$ and $2.6 \times 10^{14}$ W/cm$^2$ laser intensity, respectively. Error bars take into account laser intensity fluctuations ($\pm$10%) and pressure decay between the two measurement depths.

We now briefly comment on the possible origin of the abrupt variation of the phase noticed in Fig. 2 at late times after shock breakout. Amplitude measurements of the backscattered probe pulse performed under the experimental conditions of Fig. 2 show a strong discontinuity in reflectivity in synchronism with the drop in the phase shift seen at $\approx$50 and 80 ps after the pump pulse for the higher and lower irradiance, respectively. Experiments

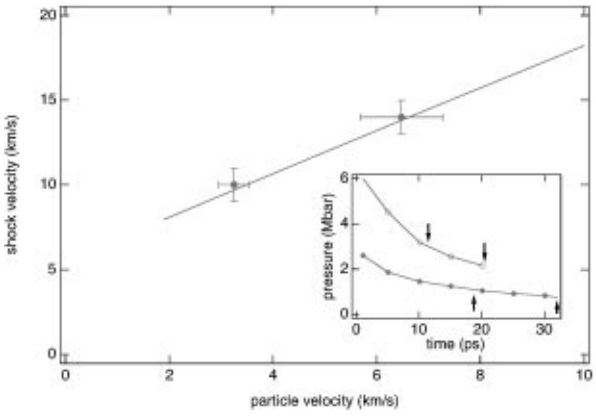


FIG. 3. Measured particle and shock velocities at $2.6 \times 10^{14}$ W/cm$^2$ (higher velocities) and $7.7 \times 10^{13}$ W/cm$^2$ (lower velocities) laser intensities. Solid line: SESAME 3717 aluminum Hugoniot curve. The inset shows the calculated shock pressure decay for these intensities. Vertical arrows show the shock breakout times for 260 nm (left) and 400 nm (right) Al thicknesses.

performed using picosecond pulses [8] that observe shock wave passage from a conducting medium into a transparent substrate show a large decrease in the reflectivity of the metallic surface during and after the arrival of the shock. This rapid decrease in the reflectivity is thought to be due to the generation and passage of an ionization front associated with the shock wave into the transparent medium. We note again that we have observed the same phenomena but at irradiances very much larger than the highest irradiance we have used here. Here we rather suspect the occurrence of pressure-induced breakdown in the dielectric where avalanche buildup of charges around dislocation damages, which can be attributed to impurity contents, is a well-known phenomena limiting the use of quartz gauges to probe multikilobar stresses in shocked materials [21].

Finally, we have exploited the unique capability of our technique to provide spatial resolution along a diameter of the pump laser focal spot to verify the planar character of subpicosecond laser-driven shock discontinuities. Truly uniaxial compression is expected in our conditions since the focal spot diameter is very much larger than the shock propagation thickness. Figure 4 shows the measured profile of the laser intensity as a function of position along one diameter of the focal spot. The phase shift registered at 40 ps after the pump laser pulse is also plotted as a function of radial position. Spatial resolution is limited by the imaging lens to about $3-5$ $\mu$m (see the error bar in Fig. 4). The aluminum thickness was 400 nm and the laser intensity $10^{14}$ W/cm$^2$. Then the MULTI code was run for each laser intensity along the diameter of the focal spot and the results were postprocessed by the multilayer program. Results (see Fig. 4) are in perfect agreement with the experiment.

In conclusion, space- and time-resolved optical probing of femtosecond laser-driven shock waves at an Al/$SiO_2$ interface have been demonstrated. Frequency-domain interferometry allows us to measure *simultaneously* shock and particle velocities at an interface with an unprecedented time resolution. Shock and interface velocities are accurately predicted by hydrodynamic simulations using a standard equation of state for Al and $SiO_2$. Pressures $P = 1-3$ Mbar are measured along the aluminum Hugoniot curve for $\sim 10^{14}$ W/cm$^2$, 120 fs laser irradiances and durations.

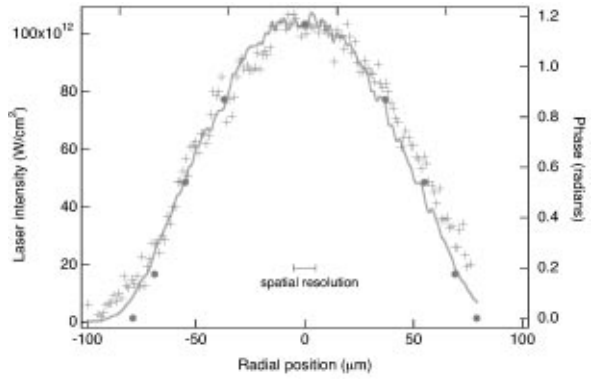


FIG. 4. Radial profile of the phase shift measured 40 ps after the pump laser for a 400 nm Al layer and $10^{14}$ W/cm$^2$ laser intensity. Solid line: measured laser intensity, crosses: measured phase shift, dots: MULTI simulations.

We gratefully acknowledge the support of the laser staff at LOA where the experiments were carried out. We thank Stephan Hüller for his help in the use of the MULTI code and Allessandro Mirone for developing the multilayer model. This work was supported by the Centre National de la Recherche Scientifique, the European Community under Large Facilities Contract CHGE-CT93-0021, and under the Human Capital and Mobility Contract CHRX-CT93-0338.

*Present address: Laboratoire d'Optique Appliquée, Batterie de l'Yvette, 91120 Palaiseau, France.

[1] T. A. Hall, in *NATO-ASI Conference on Laser Interaction with Atoms, Solids and Plasmas,* edited by R. M. More (Plenum Press, New York, 1994), and references therein.
[2] F. Cottet *et al.,* Appl. Phys. Lett. **47**, 678 (1985); R. Fabbro *et al.,* Laser Part. Beams **4**, 413 (1986); B. Faral *et al.,* Phys. Fluids **2**, 371 (1990); R. Cauble *et al.,* Phys. Rev. Lett. **70**, 2102 (1993); Th. Löwer *et al.,* Phys. Rev. Lett. **72**, 3186 (1994); M. Koenig *et al.,* Phys. Rev. Lett. **74**, 2260 (1995).
[3] For a comprehensive review, see R. Pakula and R. Sigel, Phys. Fluids **28**, 232 (1985).
[4] P. Celliers, A. Ng, G. Xu, and A. Forsman, Phys. Rev. Lett. **68**, 2305 (1992).
[5] P. Celliers and A. Ng, Phys. Rev. E **47**, 3547 (1993).
[6] A. Ng, A. Forsman, and P. Celliers, Phys. Rev. E **51**, R5208 (1995).
[7] B-T. V. Vu, A. Szoke, and O. L. Landen, Opt. Lett. **18**, 723 (1993).
[8] B-T. V. Vu, O. L. Landen, and A. Szoke, Phys. Plasmas **2**, 476 (1995), and references therein.
[9] J. P. Geindre *et al.,* Opt. Lett. **19**, 1997 (1994).
[10] C. W. Siders *et al.,* IEEE Trans. Plasma Science **24**, 301 (1996).
[11] A. Sullivan and W. E. White, Opt. Lett. **20**, 192 (1995).
[12] P. Audebert *et al.,* Phys. Rev. Lett. **73**, 1990 (1994).
[13] P. Blanc *et al.,* J. Opt. Soc. Am. **13**, 118 (1996).
[14] R. E. Setchell, J. Appl. Phys. **50**, 8186 (1979).
[15] R. Ramis, R. F. Schmalz, and J. Meyer-ter-Vehn, Comput. Phys. Commun. **49**, 475 (1988).
[16] K. S. Holian, Los Alamos National Laboratory Report No. UCID-18754-82-2, 1982 (unpublished).
[17] A. Ng *et al.,* Phys. Rev. Lett. **72**, 3351 (1994).
[18] D. F. Price *et al.,* Phys. Rev. Lett. **75**, 252 (1995).
[19] A. Rousse, Ph.D. thesis (unpublished).
[20] P. Celliers, Ph.D. thesis (unpublished).
[21] R. A. Graham, J. Appl. Phys. **46**, 1901 (1975).